HHS Public Access

Author manuscript

Science. Author manuscript; available in PMC 2022 February 17.

Published in final edited form as:

Science. 2021 December 03; 374(6572): 1252–1258. doi:10.1126/science.abj1013.

Error-prone, stress-induced 3' flap-based Okazaki fragment maturation supports cell survival

Haitao Sun[1], **Zhaoning Lu**[1], **Amanpreet Singh**[1], **Yajing Zhou**[1], **Eric Zheng**[1,2], **Mian Zhou**[1], **Jinhui Wang**[3], **Xiwei Wu**[3], **Zunsong Hu**[4], **Zhaohui Gu**[4], **Judith L. Campbell**[5], **Li Zheng**[1,*], **Binghui Shen**[1,*]

[1]Department of Cancer Genetics and Epigenetics, Beckman Research Institute, City of Hope, 1500 East Duarte Road, Duarte, CA 91010

[2]Department of Molecular, Cellular, and Developmental Biology, University of California at Santa Barbara, Santa Barbara, CA 93106

[3]Department of Molecular and Cellular Biology, Beckman Research Institute, City of Hope, 1500 East Duarte Road, Duarte, CA 91010

[4]Department of Computational and Quantitative Medicine, Beckman Research Institute, City of Hope, 1500 East Duarte Road, Duarte, CA 91010

[5]Divisions of Chemistry and Chemical Engineering and Biology and Biological Engineering California Institute of Technology, Pasadena, CA 91125, USA

Abstract

How cells with DNA replication defects acquire mutations that allow them to escape apoptosis under environmental stress is a long-standing question. Here, we report an error-prone Okazaki fragment maturation (OFM) pathway that is activated at restrictive temperatures in *rad27*Δ yeast cells. Restrictive temperature stress activates Dun1, facilitating transformation of un-processed 5' flaps into 3' flaps, which are removed by 3' nucleases including Polδ. However, at certain regions, 3' flaps form secondary structures that facilitate 3' end extension rather than degradation, producing alternative duplications with short spacer sequences. Once such mutations occur at *POL3*, it fails to displace 5'flaps, thus rescues *rad27*Δ cells. Our study defines a stress-induced, error-prone OFM pathway that generates mutations that counteract replication defects and drive cellular evolution and survival.

Understanding the mutagenesis mechanisms that are active in cells under stress conditions is crucial for developing strategies to intervene in microbial pathogenesis, tumorigenesis, and drug resistance (1, 2). Lagging-strand DNA synthesis is particularly vulnerable to stress and environmental factors. During replication, lagging-strand DNA is synthesized as

*Corresponding authors: lzheng@coh.org (L.Z.); bshen@coh.org (B.S.).

Author contributions: H. Sun, Z. Lu, A. Singh, Y. Zhou, M. Zhou conducted yeast genetic and biochemical experiments. E. Zheng, J. Wang, X. Wu, Z. Hu, and Z. Gu conducted RNA-seq, WES, and WGS and performed data analysis. J.L. Campbell designed yeast genetic experiments and conducted data analysis. L. Zheng conducted biochemical experiments, RNA-seq, and WGS data analysis, designed and coordinated most of the experiments, and wrote the first draft of the manuscript. B. Shen supervised the entire project, designed and coordinated most of the experiments, and provided input into and finalized the manuscript.

Competing interests: The authors declare no conflicts of interest in this study.

discrete Okazaki fragments (3), which contain short primase/Polα-synthesized RNA-DNA primers at their 5' ends (4-6). During Okazaki fragment maturation (OFM), the RNA portion and any Polα-synthesized DNA with high incorporation errors are removed, via Polδ-mediated displacement DNA synthesis, which produces a 5' RNA-DNA flap (4-6). The 5' flap structure is removed by flap endonuclease 1 (FEN1) or through the sequential actions of DNA2 nuclease/helicase and FEN1 (7-9). FEN1 deficiency leads to accumulation of unprocessed 5' flap structures, which may prevent ligation of Okazaki fragments, leaving DNA nicks or gaps that lead to collapse of replication forks and DNA double-strand breaks. In yeast, deletion of the FEN1 homolog *RAD27* (*rad27*)Δ results in slow growth at permissive growth temperatures (30°C) and death at restrictive growth temperatures (37°C) (10).

Nevertheless, we discovered that a small population of *rad27*Δ yeast cells, which we called revertants, could grow at a similar rate as wild-type (WT) cells at 37°C (Fig. 1A). To determine if the revertants acquired somatic mutation(s) that permitted growth and to identify any such mutation(s), we conducted whole-genome sequencing (WGS) of WT, parental *rad27*Δ, and a revertant strain of yeast cells. We identified 21 somatic DNA mutations specific to one revertant colony (Table S1). A mutation in *POL3*, the DNA polymerase delta (Polδ) catalytic subunit (11), was the only nonsynonymous mutation that had 100% allele frequency in the revertant. Subsequent DNA sequencing analysis of the *POL3* gene in independent *rad27*Δ revertant colonies (n = 31) revealed that each colony harbored a *pol3* mutation (Fig. 1B). This suggests that these *pol3* mutations, which map onto POL3 functional motifs (Fig. 1B, Supplementary text S1) and possibly affect its biochemical activities, might provide a survival advantage for *rad27*Δ cells grown under restrictive temperature stress. Furthermore, knock-in of the 458–477 internal tandem duplication (ITD) mutation, which occurred in 19 of the 31 independent colonies, or any of the four representative point mutations (R470G, R475I, A484V, and S847Y) successfully reversed the restrictive temperature-induced lethality phenotype of *rad27*Δ cells (Fig. 1C and fig. S1). *rad27*Δ cells are sensitive to methyl methanesulfonate (MMS) (10). Although *rad27*Δ revertant cells and *rad27*Δ *pol3* ITD knock-in mutant cells were resistant to a low concentration (0.005%) of MMS, they were sensitive to higher concentrations (≥0.01%) of MMS (fig. S2). We observed that *pol3* ITD cells in a WT RAD27 background were also sensitive to high concentrations of MMS (fig. S2). This at least partially explains why the *pol3* ITD could not suppress MMS-induced lethality of *rad27*Δ cells at high MMS concentrations. In addition, *pol3* ITD did not rescue the synthetic lethality that occurs in the context of *rad27*Δ coupled with deficiency of the 5' nucleases *EXO1* or *DNA2* nuclease/helicase (Tables S2, S3, Supplementary text S2).

Two types of duplications were present in the revertants: *pol3* 591–598 ITD, a previously reported classic duplication resulting from re-alignment and ligation of unprocessed 5' flaps (12), and *pol3* 458–477 ITD, which contained a 55 bp duplication with a 5 bp spacer between the duplicated units (fig. S3). We named the duplication with an intervening spacer an "alternative duplication." Both *pol3* 591–598 ITD and *pol3* 458–477 ITD resembled ITDs detected in human cancer (13-15). To determine how the alternative duplication *pol3* 458–477 ITD originated, we conducted WGS of WT and *rad27*Δ cells grown at 37°C or 30°C for 4 h. The mutation frequency of WT cells was the same at both temperatures (Fig.

2A). In contrast, restrictive temperature stress increased the mutation frequency of *rad27*Δ cells by 2-fold; in particular, the frequency of duplications and base substitutions was increased (Fig. 2A). In addition, duplication insertions in *rad27*Δ cells grown at 37°C were considerably longer than those in *rad27*Δ cells grown at 30°C (Fig. 2B). The duplications revealed that *rad27*Δ cells grown at 37°C exhibited alternative duplications that were similar to the *pol3* 458–477 ITD. The alternative duplications were not detected in WT cells (30°C or 37°C) or in *rad27*Δ cells grown at 30°C (Fig. 2C), suggesting that alternative duplications were induced by restrictive temperature stress.

We further noted that the sequences of these alternative duplications suggested formation of three different types of hairpin structures (Fig. 2D, fig. S4A-4D, Supplementary text S3). This supports a model of sequential actions, including conversion of a 5' Okazaki fragment flap to a 3' flap, annealing of the flap to a complementary sequence, extension of the 3' flap, realignment, and ligation of the extended 3' flap to produce an alternative duplication, including *pol3* 458–477 ITD. Consistent with this model, our WGS data indicated that 40% of the alternative duplications also carried base substitutions at the duplication unit. These substitutions most likely resulted from failure to remove Polα-generated errors on the 5' flap. To determine if the restrictive temperature induced 3' flap formation in *rad27*Δ cells, we developed an approach to specifically label the OH group on the 3' flap on genomic DNA, in which 3' OH at the nick or at the DNA end was pre-blocked with dideoxyribonucleotides (Fig. 2E). We detected a considerable number of 3' flaps in *rad27*Δ cells grown at 37°C; in contrast, we detected few flaps in *rad27*Δ cells grown at 30°C, in WT cells grown at either temperature, or in *rad27*Δ cells carrying *pol3* 458–477 ITD grown at either temperature (Fig. 2F). Furthermore, pre-incubation of Polδ with genomic DNA from *rad27*Δ cells grown at 37°C could effectively remove the 3' flaps (Fig. 2G), suggesting that Polδ may process 3' flaps during OFM.

To define the proposed 3' flap-based OFM mechanism, we reconstituted the sequential reactions of 3' flap cleavage, DNA synthesis, and ligation of oligo-based DNA substrates (S) with a simple 3' flap (S2 or S3; Fig. 2H and fig. S5B) or a secondary structure-forming 3' flap (S4 or S5; Fig. 2I) for formation of type I or type II alternative duplications. In the presence of deoxyribonucleotide, Polδ could effectively cleave 3' flap substrates S2 and S3 and stop at the junction of the 3' flap and DNA duplex, generating ligatable DNA nicks for DNA Lig I (Fig. 2H and fig. S5, Supplementary text S4). However, deoxyribonucleotides inhibited cleavage of hairpin-forming 3' flaps, and promoted extension of the annealed 3' flap, producing ligated extended products (Fig. 2I, Supplementary text S4); this process resembled formation of alternative duplications. When extension of the annealed 3' flap could not generate ligatable nicks, only unligatable extended products were produced (fig. S6A-6D), leading to failure of 3' flap-based OFM. The single-stranded DNA (ssDNA) binding protein RPA had little effect on Polδ-mediated 3' flap cleavage or subsequent nick ligation (Fig. 2H), and it slightly enhanced formation of the ligated extended products (Fig. 2I).

Using reconstitution assays, we showed that the 3' nuclease activities of Polδ and Lig I were sufficient to complete 3' flap processing for OFM. Other nucleases in the nuclear extract (NE) might also be important in processing 3' flaps, especially the hairpin-forming 3' flap

(fig. S7A, S7B, Supplementary text S5). However, NE from *rad27A*Δ cells, particularly those grown at 37°C, had reduced 3' flap processing activity (fig. S7A, S7B, Supplementary text S5). Because we observed no significant changes in expression of major 3' nucleases in yeast (fig. S8), we postulated that restrictive temperature stress could also induce molecular changes to inhibit 3' flap processing, allowing 3' flaps to invade into nearby homologous sequences, leading to alternative duplications.

We next determined how the *pol3* 458–477 ITD enabled *rad27*Δ cells to overcome lethal stress. Because the *pol3* 458–477 ITD did not change Polδ protein levels in *rad27*Δ cells (fig. S9), we tested if it affected biochemical properties of Polδ. We assayed the DNA polymerase and 3' nuclease activities of a purified recombinant protein Polδ complex containing either a WT Pol3 subunit (WT Polδ) or a 458–477 ITD Pol3 subunit (hereafter called Polδ-ITD). Polδ-ITD could catalyze DNA synthesis but was less processive than WT Polδ during primer extension (Fig. 3A). Similarly, Polδ-ITD could effectively fill the gap, but it was less active than WT Polδ in displacing the downstream DNA oligo (Fig. 3B). In addition, Polδ-ITD had relatively weak 3' exonuclease activity on DNA duplexes, compared to WT Polδ (fig. S10). However, Polδ-ITD had similar activity to WT Polδ in cleaving the 3' flap and generating a ligatable nick (fig. S11). This activity likely allows cells carrying the *pol3* 458–477 ITD to have a similar capacity as WT cells for catalyzing 3' flap processing for OFM. In contrast, a 3' exonuclease-dead mutant, Polδ D520E, did not cleave the 3' flap (fig. S11), which may explain why the Polδ D520E mutation is lethal at restrictive temperature and synthetically lethal with *rad27*Δ (16).

We further revealed that knock-in of*pol3* mutations significantly reduced the mutation rate of *rad27*Δ cells, as measured by Canavanine resistance (Can^r) (Fig. 3C) but did not affect the mutation rate of yeast cells with WT Rad27 (fig. S12). These *pol3* mutations nearly completely suppressed the occurrence of duplications (Fig. 3D). Consistent with the Can^r assay results, our WGS data confirmed that *pol3* mutations reduced the frequency of duplications and the overall mutation frequency (Fig. 3E). Duplication mutation rate correlates with the level of 5' flap formation (12). Thus, our biochemical and genetic results demonstrate that *pol3* ITD and other point mutations can reverse the conditional lethality phenotype by limiting 5' flap formation in *rad27*Δ cells.

To identify the signaling pathways that induced 3' flap- mediated OFM and led to generation of *pol3* ITD, we compared the transcriptomes of WT and *rad27*Δ cells grown at 37°C or 30°C. We observed that genes regulated by the checkpoint kinases Mec1, Rad53, and Dun1 were significantly up-regulated in *rad27*Δ cells, especially those grown at 37°C (Fig. 4A); consistent with this, western blot analysis confirmed that chromatin-associated Dun1 protein was increased in *rad27*Δ cells grown at 37°C (Fig. 4B). These results suggest activation of the Mec1-Rad53-Dun1 axis, the major signaling pathway that is activated to counteract genotoxic stress (17, 18). We further showed that downstream targets of the upregulated genes, including the stress response genes *HUG1, RNR2, RNR3*, and *RNR4*, and the DNA repair gene *RAD51*, were synergistically induced by *rad27*Δ and restrictive temperature stress (fig. S13). *RAD51* is associated with inhibition of 3' ssDNA degradation, which at least partially explains why degradation of 3' flaps induced by NE from *rad27*Δ cells grown at 37°C was markedly less than degradation induced by WT NE (fig. S7A, 7B).

To define the role of Dun1 signaling in stress-induced mutation and generation of revertants, we deleted the *DUN1* gene in WT and *rad27*Δ cells. We observed that knockout of *DUN1* (*dun1*)Δ in WT or *rad27*Δ cells had little effect on their survival (fig. S14), 3' flap formation (Fig. 4C), or mutation rate at 30°C (Fig. 4D). However, *DUN1* deletion markedly reduced restrictive temperature stress-induced 3' flap formation (Fig. 4C) and abolished restrictive temperature stress-induced mutations in *rad27*Δ cells (Fig. 4D). Consistent with this, *DUN1* deletion inhibited generation of *rad27*Δ revertants (Fig. 4E, Supplementary text S6). Furthermore, all *rad27*Δ revertants in this experiment had *pol3* mutations, predominantly the *pol3* 458–477 ITD, but none of the *rad27*Δ *dun1*Δ revertants had *pol3* mutations (Fig. 4F). These findings suggest that Dun1 activation plays an important role in the development of restrictive temperature stress-induced mutations that can reverse the lethal phenotype of *rad27*Δ cells. Consistent with this finding, blocking activation of Chk1, a Dun1 functional analogue, significantly inhibited spontaneous lung cancer development in FEN1 mutant mice but not in WT mice (fig. S15, Supplementary text S7). An important function of Dun1 activation is to induce overexpression of *HUG1, RNR2, RNR3*, and *RNR4* for deoxyribonucleotide production. Increased deoxyribonucleotide concentrations changed the mode of action of Polδ and promoted generation of ligated extended products *in vitro* (fig. S5, fig. S16, S17, Supplementary text S8). However, when we deleted SML1, the protein inhibitor of ribonucleotide reductase (19), to increase deoxyribonucleotide production, we did not observe increased mutation rates in *rad27*Δ cells (fig. S18), suggesting that an up-regulation of deoxyribonucleotide alone is not sufficient to promote alternative duplications.

To demonstrate the relevance of stress-induced 3' flap-based OFM and alternative duplications in *rad27*Δ cells to human cancers, we used whole-exome sequencing (WES) to analyze alternative duplications in human tumors and mutant mice modeling human FEN1 mutations. Alternative duplications, similar to those in *rad27*Δ cells grown at restrictive temperature (i.e., 3' flap OFM-related alternative duplications), were frequent in human B cell acute lymphoblastic leukemia (fig. S19A-19C, Supplementary text S9). In addition, FEN1 A159V mutation, which occurs in human lung cancers (20), promoted 3' flap OFM-related alternative duplications in mice (fig. S19D, Supplementary text S9). Therefore, mutations in FEN1 or other OFM genes may lead to 3' flap-based OFM, and play crucial roles for cancer cell evolution, tumor growth, and resistance.

Our current study defines error-prone processing of RNA-DNA primers during OFM (Fig. 4G). Induction of this mechanism generates alternative duplications and base substitutions. In WT cells, the displaced 5' RNA-DNA flap is effectively cleaved by either Rad27 alone or by Dna2, which first cleaves the 5' RNA-DNA flap in the middle, leaving a shorter 5' DNA flap for Rad27 to subsequently cleave. When Rad27 is not available, other 5' nucleases such as Dna2 alone or Exo1 are involved in inefficient 5' flap processing (21, 22). Resolution of 5' flaps also requires an alternative pathway that is mediated by the 3' exonuclease activities of Polδ, which removes nucleotides from the 3' end of an upstream Okazaki fragment, generating a gap for the unprocessed 5' flap to re-anneal for ligation (16, 23). Restrictive temperature stress activates Dun1 signaling and stimulates *de novo* production of deoxyribonucleotides, which in turn inhibits the 3' exonuclease activity, but not the flap nuclease activity of Polδ, and induces other DNA damage responses. These molecular changes push OFM toward transformation of an unprocessed 5' flap into a 3' flap,

either through flap equilibration (24) or the actions of helicases such as Sgs1 or Pif1, leading to a secondary structure that may result in alternative duplications, including Polδ-ITD, in revertant strains. In the revertants, Polδ mutations limit DNA displacement, thus suppressing 5' flap formation or allowing more time for Dna2 or Exo1 to act on the 5' flap and bypass the requirement for Rad27 (Fig. 4G).

Supplementary Material

Refer to Web version on PubMed Central for supplementary material.

Acknowledgements

We thank Dr. Richard Kolodner for the yeast strains RDKY2672, RDKY2608, RDKY2669; Dr. Peter M.J. Burgers for the plasmids pBL335 (GST-Pol3), pBL338 (GAL1-Pol31), pBL340 (GAL10-Pol32), and pBL341 (Pol31/Pol32); Drs. Louis Prakash and Satya Prakash for the protease-deficient yeast strain YRP654 and the plasmids pBJ1445 (Flag-Pol3) and pBJ1524 (GST-Pol31/Pol32) to express the yeast recombinant DNA polymerase δ complex (Pol3, Pol31, and Pol32); Dr. Wolf-Dietrich Heyer for the anti-Dun1 antibody; and Dr. Marc S. Wold for purified recombinant yeast RPA complex. We thank Huifang Dai, Daniela Duenas, and Martin E. Budd for technical assistance in mouse and yeast genetic experiments and stimulating discussions. We thank Drs. Keely Walker and Sarah Wilkinson for critical reading and editing of the manuscript.

Funding:

This work was supported by NIH grants R50 CA211397 to L.Z. and R01 CA073764 and R01 CA085344 to B.S. Research reported in this publication includes work performed by City of Hope shared resources supported by the National Cancer Institute of the National Institutes of Health under award number P30 CA033572.

Data and materials availability:

All data is available in the manuscript or the supplementary materials. Accession numbers for mouse and yeast genomics datasets are GSE181154 and GSE178876, respectively.

References and Notes

1. Fitzgerald DM, Hastings PJ, Rosenberg SM, Stress-Induced Mutagenesis: Implications in Cancer and Drug Resistance. Annu. Rev. Cancer Biol 1, 119–140 (2017). [PubMed: 29399660]
2. Galhardo RS, Hastings PJ, Rosenberg SM, Mutation as a stress response and the regulation of evolvability. Crit. Rev. Biochem. Mol. Biol 42, 399–435 (2007). [PubMed: 17917874]
3. Ogawa T, Okazaki T, Discontinuous DNA replication. Annu. Rev. Biochem 49, 421–457 (1980). [PubMed: 6250445]
4. Burgers PMJ, Kunkel TA, Eukaryotic DNA Replication Fork. Annu. Rev. Biochem 86, 417–438 (2017). [PubMed: 28301743]
5. Nick McElhinny SA, Gordenin DA, Stith CM, Burgers PM, Kunkel TA, Division of labor at the eukaryotic replication fork. Mol. Cell 30, 137–144 (2008). [PubMed: 18439893]
6. Waga S, Stillman SB. Anatomy of a DNA replication fork revealed by reconstitution of SV40 DNA replication in vitro Nature. 369, 207–212 (1994). [PubMed: 7910375]
7. Lieber MR, The FEN-1 family of structure-specific nucleases in eukaryotic DNA replication, recombination and repair. BioEssays 19, 233–240 (1997). [PubMed: 9080773]
8. Bae SH, Bae KH, Kim JA, Seo YS, RPA governs endonuclease switching during processing of Okazaki fragments in eukaryotes. Nature 412, 456–461 (2001). [PubMed: 11473323]
9. Liu Y, Kao HI, Bambara RA, Flap endonuclease 1: a central component of DNA metabolism. Annu. Rev. Biochem 73, 589–615 (2004). [PubMed: 15189154]

10. Reagan MS, Pittenger C, Siede W, Friedberg EC, Characterization of a mutant strain of Saccharomyces cerevisiae with a deletion of the RAD27 gene, a structural homolog of the RAD2 nucleotide excision repair gene. J. Bacteriol 177, 364–371 (1995). [PubMed: 7814325]
11. Sitney KC, Budd ME, Campbell JL, DNA polymerase III, a second essential DNA polymerase, is encoded by the S. cerevisiae CDC2 gene. Cell 56, 599–605 (1989). [PubMed: 2645055]
12. Tishkoff DX, Filosi N, Gaida GM, Kolodner RD, A novel mutation avoidance mechanism dependent on S. cerevisiae RAD27 is distinct from DNA mismatch repair. Cell 88, 253–263 (1997). [PubMed: 9008166]
13. Mariño-Enriquez A, Lauria A, Przybyl J, Ng TL, Kowalewska M, Debiec-Rychter M, Ganesan R, Sumathi V, George S, McCluggage WG, Nucci MR, Lee C-H, Fletcher JA, BCOR Internal Tandem Duplication in High-grade Uterine Sarcomas. Am. J. Surg. Pathol 42, 335–341 (2018). [PubMed: 29200103]
14. Kottaridis PD, Gale RE, Frew ME, Harrison G, Langabeer SE, Belton AA, Walker H, Wheatley K, Bowen DT, Burnett AK, Goldstone AH, Linch DC, The presence of a FLT3 internal tandem duplication in patients with acute myeloid leukemia (AML) adds important prognostic information to cytogenetic risk group and response to the first cycle of chemotherapy: analysis of 854 patients from the United Kingdom Medical Research Council AML 10 and 12 trials. Blood 98, 1752–1759 (2001). [PubMed: 11535508]
15. Kiyoi H, Towatari M, Yokota S, Hamaguchi M, Ohno R, Saito H, Naoe T, Internal tandem duplication of the FLT3 gene is a novel modality of elongation mutation which causes constitutive activation of the product. Leukemia 12, 1333–1337 (1998). [PubMed: 9737679]
16. Jin YH, Ayyagari R, Resnick MA, Gordenin DA, Burgers PM, Okazaki fragment maturation in yeast. II. Cooperation between the polymerase and 3'-5'-exonuclease activities of Pol delta in the creation of a ligatable nick. J. Biol. Chem 278, 1626–1633 (2003). [PubMed: 12424237]
17. Zhou Z, Elledge SJ, DUN1 encodes a protein kinase that controls the DNA damage response in yeast. Cell 75, 1119–1127 (1993). [PubMed: 8261511]
18. Zhao X, Rothstein R, The Dun1 checkpoint kinase phosphorylates and regulates the ribonucleotide reductase inhibitor Sml1. Proc. Natl. Acad. Sci. U. S. A 99, 3746–3751 (2002). [PubMed: 11904430]
19. Chabes A, Domkin V, Thelander L, Yeast Sml1, a protein inhibitor of ribonucleotide reductase. J. Biol. Chem 274, 36679–36683 (1999). [PubMed: 10593972]
20. Zheng L, Dai H, Zhou M, Li M, Singh P, Qiu J, Tsark W, Huang Q, Kernstine K, Zhang X, Lin D, Shen B, Fen1 mutations result in autoimmunity, chronic inflammation and cancers. Nat. Med 13, 812–819 (2007). [PubMed: 17589521]
21. Bae SH, Seo YS, Characterization of the enzymatic properties of the yeast dna2 Helicase/endonuclease suggests a new model for Okazaki fragment processing. J. Biol. Chem 275, 38022–38031 (2000). [PubMed: 10984490]
22. Tran PT, Erdeniz N, Dudley S, Liskay RM, Characterization of nuclease-dependent functions of Exo1p in Saccharomyces cerevisiae. DNA Repair (Amst) 1, 895–912 (2002). [PubMed: 12531018]
23. Jin YH, Obert R, Burgers PM, Kunkel TA, Resnick MA, Gordenin DA, The 3'-->5' exonuclease of DNA polymerase delta can substitute for the 5' flap endonuclease Rad27/Fen1 in processing Okazaki fragments and preventing genome instability. Proc. Natl. Acad. Sci. U. S. A 98, 5122–5127 (2001). [PubMed: 11309502]
24. Liu Y, Zhang H, Veeraraghavan J, Bambara RA, Freudenreich CH, Saccharomyces cerevisiae flap endonuclease 1 uses flap equilibration to maintain triplet repeat stability. Mol. Cell Biol 24, 4049–4064 (2004). [PubMed: 15082797]
25. Toulmay A, Schneiter R, A two-step method for the introduction of single or multiple defined point mutations into the genome of Saccharomyces cerevisiae. Yeast (Chichester, England) 23, 825–831 (2006).
26. Budd ME, Campbell JL, A yeast replicative helicase, Dna2 helicase, interacts with yeast FEN-1 nuclease in carrying out its essential function. Mol. Cell. Biol 17, 2136–2142 (1997). [PubMed: 9121462]

27. Tishkoff DX, Boerger AL, Bertrand P, Filosi N, Gaida GM, Kane MF, Kolodner RD, Identification and characterization of Saccharomyces cerevisiae EXO1, a gene encoding an exonuclease that interacts with MSH2. Proc. Natl. Acad. Sci. U. S. A 94, 7487–7492 (1997). [PubMed: 9207118]
28. Coluccio AE, Rodriguez RK, Kernan MJ, Neiman AM, The yeast spore wall enables spores to survive passage through the digestive tract of Drosophila. PLoS One 3, e2873 (2008). [PubMed: 18682732]
29. Treco DA, Winston F, Growth and manipulation of yeast. Curr. Protoc. Mol. Biol Chapter 13, Unit 13 12 (2008).
30. Reenan RA, Kolodner RD, Characterization of insertion mutations in the Saccharomyces cerevisiae MSH1 and MSH2 genes: evidence for separate mitochondrial and nuclear functions. Genetics 132, 975–985 (1992). [PubMed: 1334021]
31. Lea DE, Coulson CA, The distribution of the numbers of mutants in bacterial populations. J. Genet 49, 264 (1949). [PubMed: 24536673]
32. Zheng L, Dai H, Hegde ML, Zhou M, Guo Z, Wu X, Wu J, Su L, Zhong X, Mitra S, Huang Q, Kernstine KH, Pfeifer GP, Shen B, Fen1 mutations that specifically disrupt its interaction with PCNA cause aneuploidy-associated cancer. Cell Res. 21, 1052–1067 (2011). [PubMed: 21383776]
33. Liu S, Lu G, Ali S, Liu W, Zheng L, Dai H, Li H, Xu H, Hua Y, Zhou Y, Ortega J, Li GM, Kunkel TA, Shen B, Okazaki fragment maturation involves alpha-segment error editing by the mammalian FEN1/MutSalpha functional complex. EMBO J. 34, 1829–1843 (2015 [PubMed: 25921062]
34. Johnson RE, Prakash L, Prakash S, Pol31 and Pol32 subunits of yeast DNA polymerase delta are also essential subunits of DNA polymerase zeta. Proc. Natl. Acad. Sci. U. S. A 109, 12455–12460 (2012). [PubMed: 22711820]
35. Johnson RE, Prakash L, Prakash S, Yeast and human translesion DNA synthesis polymerases: expression, purification, and biochemical characterization. Meth. Enzymol 408, 390–407 (2006).
36. Burgers PM, Gerik KJ, Structure and processivity of two forms of Saccharomyces cerevisiae DNA polymerase delta. J. Biol. Chem 273, 19756–19762 (1998). [PubMed: 9677406]
37. Zheng L, Li M, Shan J, Krishnamoorthi R, Shen B, Distinct roles of two Mg2+ binding sites in regulation of murine flap endonuclease-1 activities. Biochemistry 41, 10323–10331 (2002). [PubMed: 12162748]
38. Zheng L, Zhou M, Guo Z, Lu H, Qian L, Dai H, Qiu J, Yakubovskaya E, Bogenhagen DF, Demple B, Shen B, Human DNA2 is a mitochondrial nuclease/helicase for efficient processing of DNA replication and repair intermediates. Mol. Cell 32, 325–336 (2008). [PubMed: 18995831]
39. Quan Y, Xia Y, Liu L, Cui J, Li Z, Cao Q, Chen XS, Campbell JL, Lou H, Cell-Cycle-Regulated Interaction between Mcm10 and Double Hexameric Mcm2-7 Is Required for Helicase Splitting and Activation during S Phase. Cell Rep. 13, 2576–2586 (2015). [PubMed: 26686640]
40. Cao B, Wu X, Zhou J, Wu H, Liu L, Zhang Q, DeMott MS, Gu C, Wang L, You D, Dedon PC, Nick-seq for single-nucleotide resolution genomic maps of DNA modifications and damage. Nucleic Acids Res. 48, 6715–6725 (2020). [PubMed: 32484547]
41. Sriramachandran AM, Petrosino G, Mendez-Lago M, Schafer AJ, Batista-Nascimento LS, Zilio N, Ulrich HD, Genome-wide Nucleotide-Resolution Mapping of DNA Replication Patterns, Single-Strand Breaks, and Lesions by GLOE-Seq. Mol. Cell 78, 975–985 e977 (2020). [PubMed: 32320643]
42. Robinson MD, McCarthy DJ, Smyth GK, edgeR: a Bioconductor package for differential expression analysis of digital gene expression data. Bioinformatics 26, 139–140 (2010). [PubMed: 19910308]
43. Jaehnig EJ, Kuo D, Hombauer H, Ideker TG, Kolodner RD, Checkpoint kinases regulate a global network of transcription factors in response to DNA damage. Cell Rep. 4, 174–188 (2013). [PubMed: 23810556]
44. Falcon S, Gentleman R, Using GOstats to test gene lists for GO term association. Bioinformatics 23, 257–258 (2007). [PubMed: 17098774]
45. Koboldt DC, Chen K, Wylie T, Larson DE, McLellan MD, Mardis ER, Weinstock GM, Wilson RK, Ding L, VarScan: variant detection in massively parallel sequencing of individual and pooled samples. Bioinformatics 25, 2283–2285 (2009). [PubMed: 19542151]

46. Ye K, Schulz MH, Long Q, Apweiler R, Ning Z, Pindel: a pattern growth approach to detect break points of large deletions and medium sized insertions from paired-end short reads. Bioinformatics 25, 2865–2871 (2009). [PubMed: 19561018]

47. Gu Z, Churchman ML, Roberts KG, Moore I, Zhou X, Nakitandwe J, Hagiwara K, Pelletier S, Gingras S, Berns H, Payne-Turner D, Hill A, Iacobucci I, Shi L, Pounds S, Cheng C, Pei D, Qu C, Newman S, Devidas M, Dai Y, Reshmi SC, Gastier-Foster J, Raetz EA, Borowitz MJ, Wood BL, Carroll WL, Zweidler-McKay PA, Rabin KR, Mattano LA, Maloney KW, Rambaldi A, Spinelli O, Radich JP, Minden MD, Rowe JM, Luger S, Litzow MR, Tallman MS, Racevskis J, Zhang Y, Bhatia R, Kohlschmidt J, Mrozek K, Bloomfield CD, Stock W, Kornblau S, Kantarjian HM, Konopleva M, Evans WE, Jeha S, Pui CH, Yang J, Paietta E, Downing JR, Relling MV, Zhang J, Loh ML, Hunger SP, Mullighan CG, PAX5-driven subtypes of B-progenitor acute lymphoblastic leukemia. Nat Genet. 51, 296–307 (2019). [PubMed: 30643249]

48. Fairfield H, Gilbert GJ, Barter M, Corrigan RR, Curtain M, Ding Y, D'Ascenzo M, Gerhardt DJ, He C, Huang W, Richmond T, Rowe L, Probst FJ, Bergstrom DE, Murray SA, Bult C, Richardson J, Kile BT, Gut I, Hager J, Sigurdsson S, Mauceli E, Di Palma F, Lindblad-Toh K, Cunningham ML, Cox TC, Justice MJ, Spector MS, Lowe SW, Albert T, Donahue LR, Jeddeloh J, Shendure J, Reinholdt LG, Mutation discovery in mice by whole exome sequencing. Genome Biol. 12, R86 (2011). [PubMed: 21917142]

49. Kent WJ, BLAT--the BLAST-like alignment tool. Genome Res. 12, 656–664 (2002). [PubMed: 11932250]

50. Zheng L, Jia J, Finger LD, Guo Z, Zer C, Shen B, Functional regulation of FEN1 nuclease and its link to cancer. Nucleic Acids Res. 39, 781–794 (2011). [PubMed: 20929870]

51. Jackson JR, Gilmartin A, Imburgia C, Winkler JD, Marshall LA, Roshak A, An Indolocarbazole Inhibitor of Human Checkpoint Kinase (Chk1) Abrogates Cell Cycle Arrest Caused by DNA Damage. Cancer Res. 60, 566–572 (2000). [PubMed: 10676638]

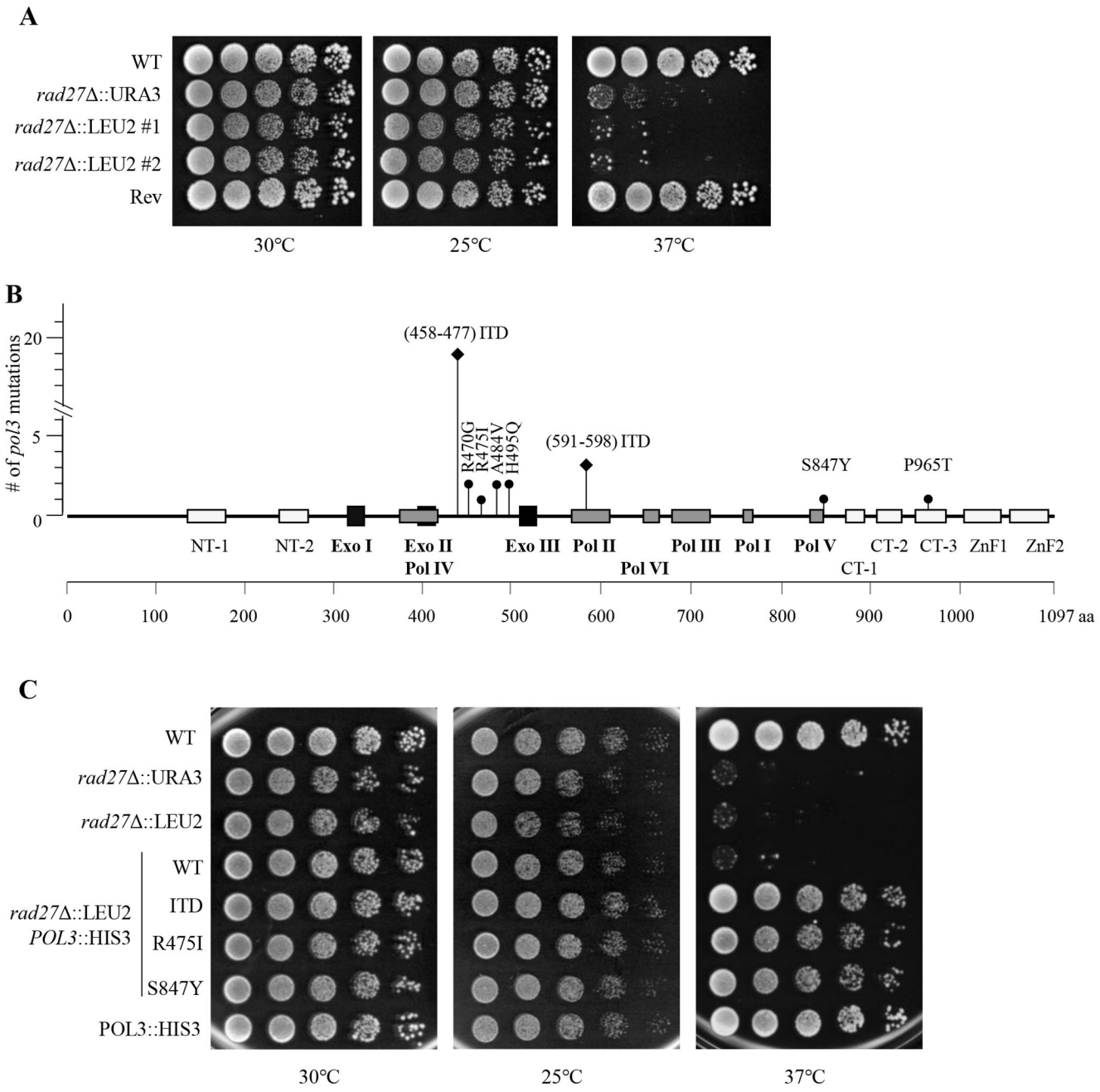

Fig. 1. Polδ internal tandem duplication (ITD) and missense mutations drive resistance to *rad27*Δ-induced conditional lethality.

(A) Spot assays of WT, *rad27*Δ, or *rad27*Δ revertant (Rev) yeast cells grown at 30°C (optimal temperature), 25°C (sub-optimal temperature), or 37°C (restrictive temperature) for 48 h. *rad27*Δ::URA3 and *rad27*Δ::LEU2 represent the *rad27*Δ allele with a linked URA3 or LEU2 selection marker gene, respectively. **(B)** *pol3* mutations detected in independent revertant strains (n=31). Circles and diamonds represent base substitution and ITD mutations, respectively. The domain structures were defined as previously described (23). **(C)** Spot assays of WT, *rad27*Δ, or *rad27*Δ yeast cells with indicated *pol3* knock-in

mutations grown at 30°C, 25°C, or 37°C for 48 h. POL3::HIS3 represents the POL3 (WT or mutant) alleles with a linked HIS3 selection marker gene.

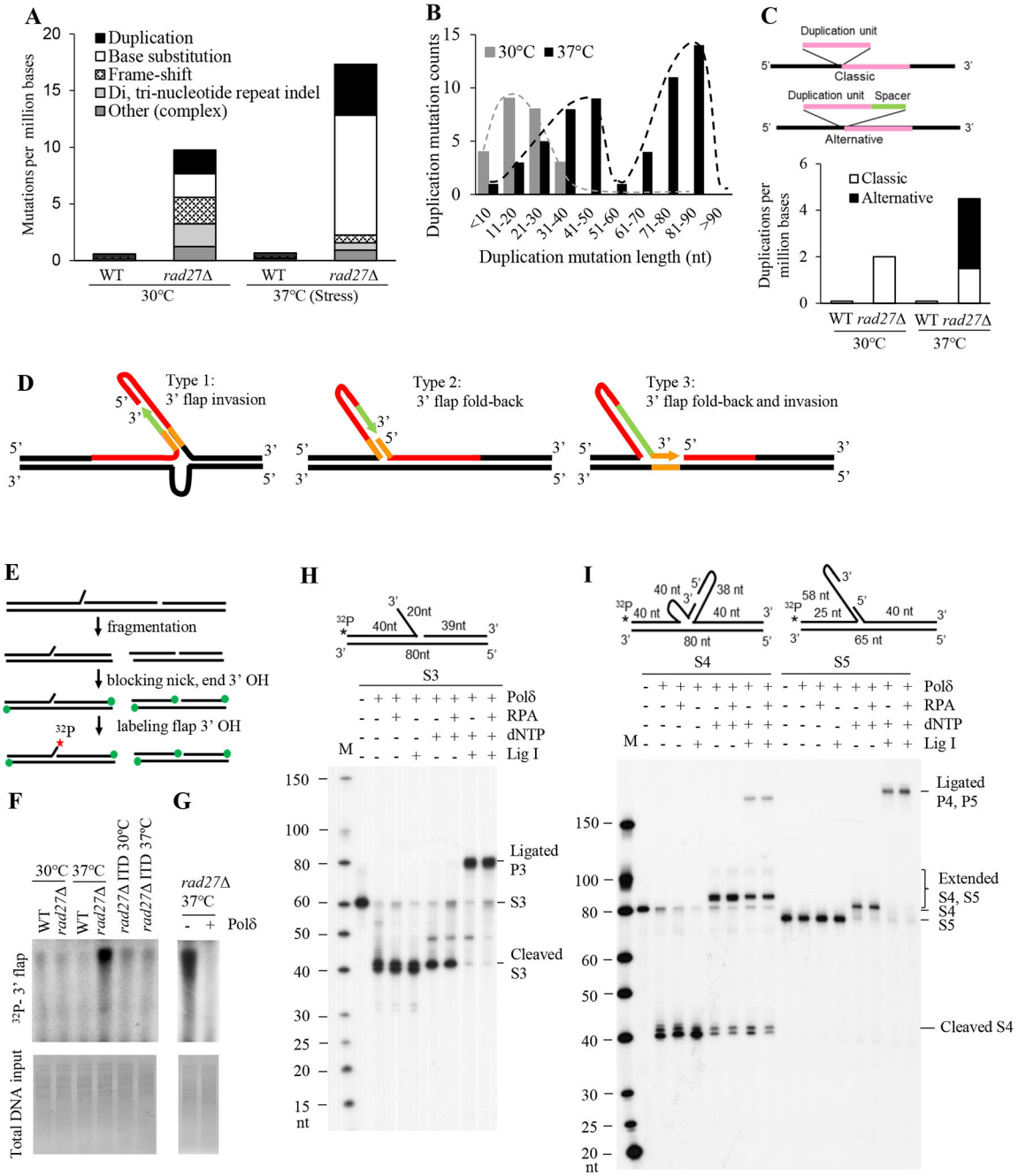

Fig. 2. Restrictive temperature stress induces 3' flap-based OFM and results in alternative duplications.

(A) Somatic mutation frequencies and types as determined by WGS, in WT and *rad27*Δ cells grown at 30°C or 37°C for 4 h. **(B)** Lengths of inserted DNA sequences in duplications in *rad27*Δ cells grown at 30°C or 37°C for 4 h. **(C)** Top, diagram of classic and alternative duplications. Bottom, frequencies of classic and alternative duplications. **(D)** Predicted structures leading to three types of alternative duplications. Red and green lines: DNA sequences in red and green in fig. S4A; Orange lines: yellow highlighting in

fig. S4A. **(E)** Schematic for specific labeling of 3’ flaps in genomic DNA. Green dots: dideoxyribonucleotide; red star: ^{32}P-deoxyribonucleotide. **(F)** Levels of 3’ flaps in genomic DNA from WT, *rad27*Δ, or *rad27*Δ pol3 ITD (*rad27*Δ-ITD) cells grown at 30°C or 37°C for 4 h. **(G)** Levels of 3’ flaps in genomic DNA from *rad27*Δ cells grown at 37°C with or without pre-treatment with Polδ. **(H and I)** Reconstitution assays using ^{32}P-labeled 3’ flap substrate S3 (**H**) or ^{32}P-labeled secondary structure-forming 3’ flap substrate S4 or S5 (**I**). Substrate structures are shown above a representative image of 8% denaturing PAGE. DNA substrates (S3, S4, S5), cleavage products (Cleaved S3, S4), unligated extended 3’ flap intermediates (Extended S4, S5), and ligated extended products (Ligated P3, P4, P5) are indicated. dNTP: deoxyribonucleotides.

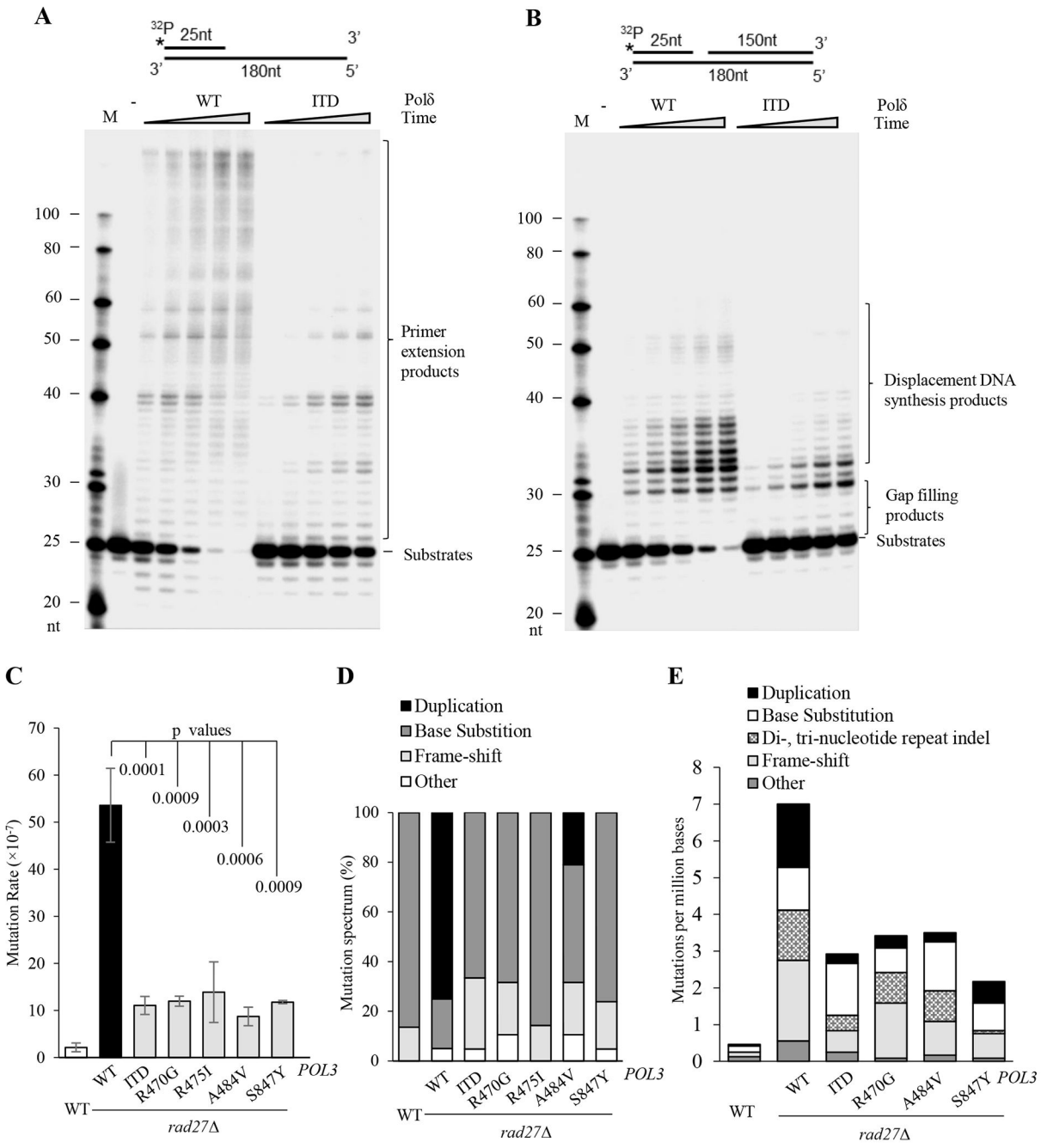

Fig. 3. Polδ-ITD suppresses 5' flap formation.

(A and B) *In vitro* assays of primer extension **(A)** and displacement DNA synthesis **(B)** by WT Polδ or Polδ-ITD. DNA substrates and primer extension products in panel A, and DNA substrates, gap filling products, or displacement DNA synthesis products in panel B are indicated. **(C)** Mean Can^r mutation rates of WT (n=5), *rad27*Δ (n=5), or *rad27*Δ yeast cells with knock-in of *pol3* 458-477 ITD (n=3), *pol3* R470G (n=2), *pol3* R475I (n=3), *pol3* A484V (n=2), and *pol3* S847Y (n=2). Error bars indicate s.d. p values were calculated using student's t test. **(D)** Can^r mutation spectra of the indicated yeast strains. Values shown are

percentages of the specific type of Can^r mutation in WT (*n*=22), *rad27*Δ (*n*=20), *rad27*Δ with knock-in of *pol3* 458-477 ITD (*n*=21), *pol3* R470G (*n*=10), *pol3* R475I (*n*=21), *pol3* A484V (*n*=19), or *pol3* S847Y (*n*=21). **(E)** Mutation frequencies and types present across the genome, as determined by WGS, in WT, *rad27*Δ, or *rad27*Δ cells with indicated *pol3* knock-in mutations grown at 30°C (*n*=1).

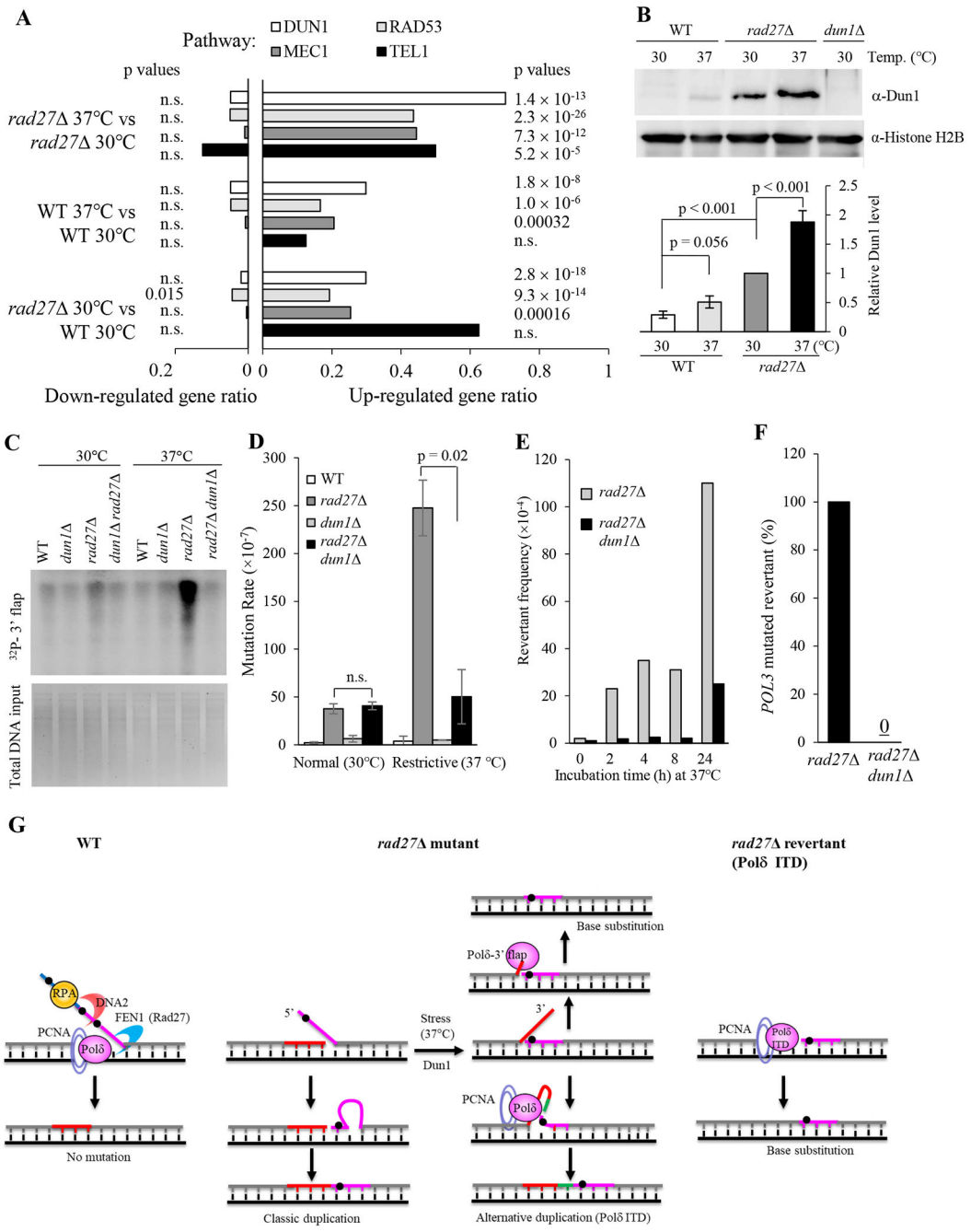

Fig. 4. Restrictive temperature stress activates signaling that facilitates error-prone OFM and generation of *rad27*Δ revertants.

(A) Up-regulated or down-regulated gene ratios in Dun1-, Rad53-, Mec1-, or Tell-controlled pathways in WT or *rad27*Δ yeast cells exposed to 30°C (4 h) or 37°C (4 h). p values were calculated using the hypergeometric test; n.s., not significant. **(B)** Top, western blot of chromatin-associated Dun1 protein in WT or *rad27*Δ cells exposed to 30°C (4 h) or 37°C (4 h). Histone H2B was used as a loading control for the chromatin fraction in each sample. *dun1*Δ is a negative control. Bottom, quantification of chromatin-associated

Dun1 relative to the loading control. The Dun1 level in *rad27*Δ cells grown at 30°C was arbitrarily set as 1, and the relative Dun1 levels in other samples were calculated by dividing their Dun1 levels by that in *rad27*Δ cells grown at 30°C. Error bars indicate s.e.m (n=4 biological replicates). **(C)** Levels of 3' flaps in genomic DNA from WT, *dun1*Δ, *rad27*Δ, or *rad27*Δ *dun1*Δ double-mutant cells grown at 30°C or 37°C for 4 h. **(D)** Mean Can^r mutation rates of WT, *rad27*Δ, *dun1*Δ, and *rad27*Δ *dun1*Δ cells exposed to 30°C (4 h) or 37°C (4 h). Error bars indicate s.d. (n=3 independent assays). **(E)** Median revertant frequencies of *rad27*Δ or *rad27*Δ *dun1*Δ cells (n=3 independent assays). **(F)** Percentage of *rad27*Δ or *rad27Δ dun1*Δ revertants that carry a *pol3* mutation (n=19 for each strain). **(G)** Schematic illustrating error-free 5' flap-mediated OFM in WT cells, error-prone 3' flap-mediated OFM and the corresponding consequences in *rad27*Δ cells under restrictive temperature stress (37°C), and the impact of Polδ-ITD on OFM in the revertant. Blue and pink segments, primase/Polα-synthesized RNA primer and DNA. Red segment, Polδ-synthesized DNA, replacing Polα-synthesized DNA. Green segment, Polδ-synthesized spacer DNA as part of alternative duplication. Black dots, Polα incorporation errors.